Engineering Solutions to Mechanics, Marine Structures and Infrastructures

Eng. Solut. Mech. Mar. Struct. Infrastruct.
2025.2(1).1
ISSN：3006-2837
https://doi.org/10.58531/esmmsi/2/1/1

Original Research

The Impact of Marine Mooring Cable Material Composition on Mooring Mechanical Performance

Yihao Zhang, Yutao Tian, Jiayan Lin, Dapeng Zhang*

Ship and Maritime college, Guangdong Ocean University, Zhanjiang 524088, China

Academic Editor: Weiwei Wang <zhwangww@ytu.edu.cn>
Received: 2 January 2025; Revised: 28 January 2025; Accepted: 31 January 2025; Published: 4 February 2025

Abstract: Marine cables play an irreplaceable role in securing floating offshore structures. The mechanical properties of mooring cables during the mooring process are crucial for ensuring the stable operation of floating offshore structures. The mechanical properties of mooring cables are primarily influenced by their material characteristics, which are mainly reflected in three key parameters: Poisson's ratio, linear density, and elastic modulus. In light of this, this study, based on the specific marine environmental parameters of a certain sea area, discretizes the mooring cable into a lumped mass parameter model and utilizes a time-domain simulation model to analyze the dynamic response of the mooring cable in the time domain. This approach further explores the impact of different Poisson's ratios, linear densities, and elastic moduli on the mooring mechanical performance of the mooring cable. The simulation results indicate that, under the assumption of an infinitely large bulk modulus, changes in Poisson's ratio have a relatively minor impact on the mechanical performance of the mooring cable. As the linear density of the mooring cable increases, the mooring tension experienced by the cable correspondingly increases, and the spatial configuration of the cable also undergoes significant changes. Moreover, variations in the elastic modulus significantly affect the dynamic configuration and mooring mechanical performance of the mooring cable.

Keywords: Mooring Cable; Poisson's Ratio; Linear Density; Elastic Modulus; Mooring Mechanical Performance

1. Introduction

In the analysis of deep-sea moored floating bodies, the dynamic response of mooring cables significantly influences the behavior of the floating bodies. Within the realm of offshore oil development, anchor systems, distinguished by their simplicity, reliable

Citation: Zhang Y., Tian Y., Lin J., Zhang D. Title. Eng. Solut. Mech. Mar. Struct. Infrastruct., 2025, 2(1), doi: 10.58531/esmmsi/2/1/1

positioning, and economic viability, continue to play a pivotal role in the positioning of offshore platforms. The dynamic performance of the anchor line holds substantial implications for the design, safety, and operational aspects of the platform's anchoring system. The coupled motion of moored floating bodies encompasses three principal components: hydrodynamic modeling of the floating body, mechanical analysis modeling of the mooring cable, and the coupling algorithm of the mooring cable. As discussed by JACOB et al. [1], coupling algorithms can be categorized into "strong coupling" and "weak coupling" methodologies. The "strong coupling" approach integrates the dynamics equations of the floating body and the mooring line through spring forces (moments) and damping forces (moments), thereby forming a multi-degree-of-freedom equation set that concurrently resolves the dynamics system of the floating body and the slender rod, treating the floating body and mooring cable as an integrated entity for solution. In contrast, the "weak coupling" method involves the independent resolution of the dynamics modules of the floating body and the flexible rod, with coupling achieved through the exchange of displacement and force data. RAN [2] and GARRET [3] have respectively developed time-domain fully coupled dynamic analysis programs. KIM et al. [4] incorporated the nonlinear mathematical model of polyester cable material into the motion and control equations of the mooring cable, conducting a coupled analysis with a deep-sea platform. Zhang et al. [5] utilized quasi-static coupling, semi-coupling, and full coupling methods to numerically simulate a Spar platform, subsequently comparing the outcomes with experimental data. Building upon the asynchronous coupling method proposed by Jing et al. [6], Ma Shan et al. [7-9] developed a dynamic coupling analysis program for the interaction between deep-sea floating bodies and their mooring and riser systems, which has been effectively validated in the dynamic response analysis of single-point mooring FPSOs and Spar platforms. This approach falls under the "weak coupling" category, and due to the mooring system being resolved as a distinct module, it is particularly amenable to parallel computation strategies. Ryu Sangsoo et al [10] undertook extensive experimental and numerical calculation research on deep-water offloading buoy systems.

In summary, a considerable amount of research has been conducted by scholars both domestically and internationally on the positioning technology of mooring systems [11-13]. Consequently, as the development of offshore oil exploitation continues to advance into deeper waters, and in light of the increasing awareness of risks and the heightened demands for reliability assessments in offshore oil engineering, the dynamic analysis of mooring lines is gaining increasing significance.

Upon comparative analysis, it has been observed that research on the impact of mooring cable material composition on the mooring mechanical performance of such cables is relatively sparse both domestically and internationally. Consequently, it is imperative to

conduct studies focusing on how the material properties of mooring cables influence their mooring mechanical performance.

In light of this necessity, this paper presents a simulation analysis examining the influence of variations in the linear density, Poisson's ratio, and elastic modulus of mooring cables on their dynamic characteristics during the mooring process. Valuable conclusions have been drawn from this analysis, which hold significant implications for guiding specific marine engineering practices.

2. **Theory**

Marine mooring cables are a typical type of slender flexible marine components. Before conducting dynamic simulations of these slender flexible marine components, they must first achieve static equilibrium to obtain their configuration at static balance. Therefore, the calculation for the static equilibrium phase must be performed initially. The method for calculating the static equilibrium of slender flexible marine components is the catenary method. A brief introduction to this method is provided below.

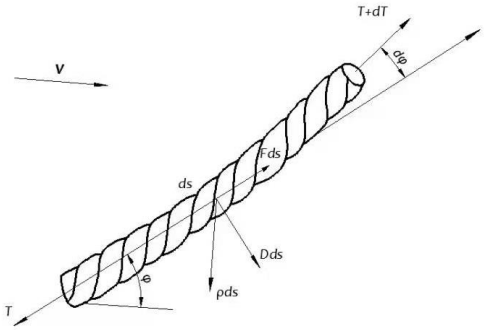

Figure.1. Schematic diagram of the force on a mooring cable element.

Consider a small element d*s* of the mooring cable as the object of study, as shown in Figure 1.Here, *D* and *F* represent the fluid forces per unit length acting in the vertical and tangential directions of the cable element, respectively ;*T* is the tension in the mooring cable; Φ is the angle between the mooring cable element and the direction of the water flow, known as the mooring cable angle; d*T* and d*Φ* are the small increments of tension and the mooring cable angle ΦΦ on the cable element d*s*; *w* is the weight per unit length of the mooring cable in water, i.e., the weight of the cable after deducting the buoyancy. Since the ends of the mooring cable element d*s* are not actually subjected to fluid pressure, and the buoyancy of the cable element is calculated based on its displaced volume with the end fluid pressures already accounted for, a correction term should be introduced in the force analysis of the mooring cable element. That is, as shown in the Figure 1., the terms $\rho gA(h-z-\mathrm{d}z)$ and $\rho gA(h-z)$ should be subtracted from the tensions at the upper and lower ends of the mooring cable element, respectively, where *A* is the cross-sectional area of the mooring cable.

From Figure 1, it can be seen that when these forces are in static equilibrium, the following equation relationships hold:

In the normal direction of the mooring cable element,

$$T\,\mathrm{d}\phi - \rho g A(h-z)\,\mathrm{d}\phi = (w\cos\phi + D)\mathrm{d}s \tag{1}$$

In the tangential direction,

$$\mathrm{d}T - \rho g A\mathrm{d}z = (w\sin\phi - F)\mathrm{d}s \tag{2}$$

In the aforementioned equations, the premise that the changes in tension dT and the mooring cable angle dΦ along the cable element are small quantities is utilized, and terms containing higher-order small quantities such as dTdΦ , dzdΦ , etc., are neglected.

If the apparent tension T' is introduced, defined as $T'=T-\rho gA(h-z)$, then the two equations can be respectively represented as:

$$T\mathrm{d}\phi = (w\cos\phi + D)\mathrm{d}s \tag{3}$$

$$\mathrm{d}T = (w\sin\phi - F)\,\mathrm{d}s \tag{4}$$

For the sake of brevity in expression, the prime symbol on T is omitted.

The two mooring cable equilibrium equations mentioned above are nonlinear, and it is impossible to find analytical solutions. However, under certain conditions, seeking analytical solutions is feasible. If the mooring cable is made of a heavier material or the sea current velocity is relatively low, the forces acting on the mooring cable are primarily dominated by gravity, and the fluid forces can be neglected. Equations (3) and (4) can then be simplified to:

$$T\mathrm{d}\phi = w\cos\phi\mathrm{d}s \tag{5}$$

$$\mathrm{d}T = w\sin\phi\,\mathrm{d}s \tag{6}$$

Dividing equation (5) by equation (6) yields:

$$\ln\frac{T}{T_0} = \int_{\phi_0}^{\phi}\tan\phi\,\mathrm{d}\phi = \ln\sec\phi\,|_{\phi_0}^{\phi} = \ln\frac{\cos\phi_0}{\cos\phi} \tag{7}$$

Hence, we obtain：

$$T = T_0\frac{\cos\phi_0}{\cos\phi} \tag{8}$$

Among them, T is the tension of the mooring cable when the mooring cable angle is Φ_0.

Substituting equation (8) into equation (5), and integrating from the origin to the cable length s_0 to s (with the cable angles at the two points being Φ_0 and Φ respectively), we can obtain:

$$s - s_0 = \int_{\phi_0}^{\phi} \frac{T_0 \cos\phi_0}{w\cos^2\phi} \mathrm{d}\phi = \frac{T_0 \cos\phi_0}{w} (\tan\phi - \tan\phi_0) \tag{9}$$

Let $T_\mathrm{h}=T_0\cos\Phi_0$，then we have:

$$s - s_0 = \int_{\phi_0}^{\phi} \frac{T_0 \cos\phi_0}{w\cos^2\phi} \mathrm{d}\phi = \frac{T_\mathrm{h}}{w} (\tan\phi - \tan\phi_0) \tag{10}$$

Along the direction of the cable, we have $\mathrm{d}x=\mathrm{d}s\cos\Phi$，Substituting this into equation (5), we can obtain:

$$x - x_0 = \int_{\phi_0}^{\phi} \frac{T_0 \cos\phi_0}{w\cos\phi} \mathrm{d}\phi = \frac{T_\mathrm{h}}{w} [\ln(\frac{1}{\cos\phi} + \tan\phi) - \ln(\frac{1}{\cos\phi_0} + \tan\phi_0)] \tag{11}$$

Similarly, along the direction of the cable, we have $\mathrm{d}z=\mathrm{d}s\sin\Phi$，Substituting this into equation (5), we can obtain:

$$z - z_0 = \int_{\phi_0}^{\phi} \frac{T_0 \cos\phi_0 \sin\phi}{w\cos^2\phi} \mathrm{d}\phi = \frac{T_\mathrm{h}}{w} (\frac{1}{\cos\phi} - \frac{1}{\cos\phi_0}) \tag{12}$$

Equations (11) and (12) represent the expressions for the cable length, horizontal distance, and vertical distance between any two points during the static equilibrium phase of the mooring cable. If the lower limit of integration is taken at the origin, then we have:

$$\frac{w}{T_\mathrm{h}} x = \ln(\frac{1+\sin\phi}{\cos\phi}) \tag{13}$$

If we let $a=T_\mathrm{h}/w$，then we have：

$$\frac{x}{a} = \ln(\frac{1+\sin\phi}{\cos\phi}) \tag{14}$$

Hence, we obtain：

$$\sinh\frac{x}{a} = \tan\phi \tag{15}$$

$$\cos \mathrm{h} \frac{x}{a}=\frac{1}{\cos \phi} \tag{16}$$

Thus, equations (10) and (12) can be written as:

$$s=a \sinh \frac{x}{a} \tag{17}$$

$$z=a(\cosh \frac{x}{a}-1) \tag{18}$$

Equations (17) and (18) are known as the catenary equations.

From equations (17) and (18), we can obtain:

$$(z+a)^2=s^2+a^2 \tag{19}$$

$$s=\sqrt{z(z+2a)} \tag{20}$$

$$x=a \cosh ^{-1}(\frac{z}{a}+1) \tag{21}$$

The above process is the derivation of the traditional catenary method, which is based on the assumption that gravity can be neglected compared to fluid forces. This method yields a definite analytical solution, and thus it can be referred to as the analytical catenary method. The shape of the mooring cable in the static equilibrium phase in this paper is derived based on the aforementioned theory.

3. **Establishment of the computational model**

Currently, the most commonly used modeling and discretization method for slender flexible components such as marine cables are the lumped mass method, the accuracy of which has been widely verified. Therefore, in this paper, the lumped mass method is used to model the marine mooring cable. For detailed information on the lumped mass method, please refer to the detailed discussion in Reference [14], which will not be repeated here. The upper end of the mooring cable is fixed at the sea surface, and the lower end is anchored to the seabed, with an initial catenary shape.

The marine environmental parameters are as follows: the seawater density is 1025kg/m³, the water depth is 100m, there is no wind or current, the wave direction is 180°, the wave height is 7m, the wave period is 8s, and the wave theory is the Dean Stream theory. The cable length is 150 m, each segment is 5m, the outer diameter of the cable is 0.35m, the inner diameter is 0.25m, and the drag coefficient is 1.2.The selection of

Poisson's ratio (0.2–0.5), linear density (0.16–0.18 t/m), and elastic modulus (100–100,000 Pa) was based on ISO 19901-7:2019 standards for offshore mooring systems [15], which recommend these ranges to cover typical material properties of synthetic and steel cables in marine environments.

When calculating the influence of different elastic moduli on the calculation results, the linear density of the cable is taken as 0.18t/m, and the Poisson's ratio is taken as 0.2. When calculating the influence of different linear densities on the calculation results, the Poisson's ratio is taken as 0.5. When calculating the influence of different Poisson's ratios on the calculation results, the linear density of the cable is taken as 0.18t/m. To validate the simulation model, a comparison between the simulated tension values and experimental data from [16] was conducted. The results showed a maximum deviation of 5.2% in top-end tension under wave height 7m, indicating good agreement between the numerical model and physical experiments.

4. **Computational results**

4.1 The influence of poisson's ratio on the mechanical properties of mooring cables

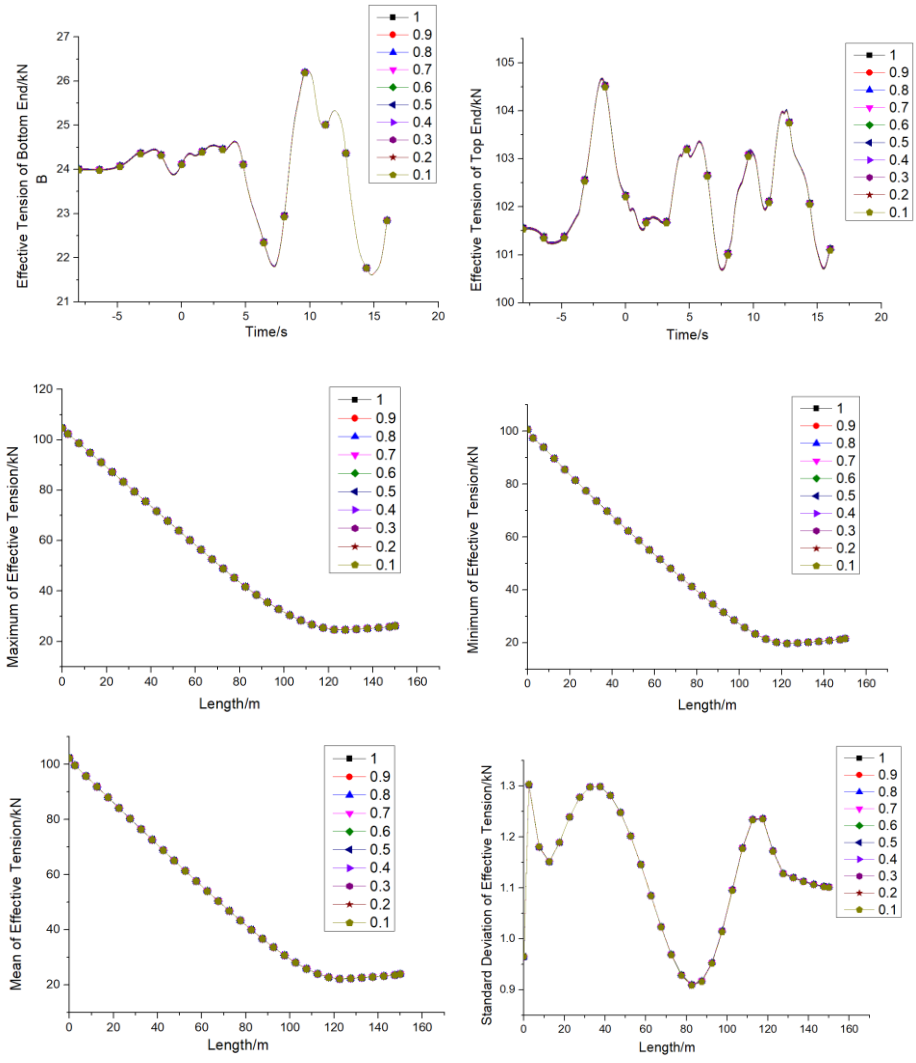

Figure.2. Variation of Effective Tension in Cables with Different Poisson's Ratios.

Just as shown in Figure 2,upon examining the variation in the effective tension of cables under different Poisson's ratios, it is evident that the influence of Poisson's ratio on the effective tension of cables is minimal, with the curves of effective tension under different Poisson's ratios being highly coincident. However, it is observed that under constant sea conditions and with other cable parameters held constant, the effective tension at the top end of the cable is consistently greater than that at the bottom end. A comparative analysis of the maximum, minimum, and average values of the effective tension along the length of the cable reveals that the effective tension increases as one approaches the top end of the cable. The distribution of the standard deviation of the effective tension along the cable's length indicates that the degree of fluctuation in effective tension varies along the cable. Specifically, within the 0-5m range, the fluctuation in mooring tension increases linearly; between 5m and 10m, the intensity of tension fluctuations gradually diminishes; from 10m to 30m, there is a trend of increasing fluctuation, reaching a maximum at 30m, where the degree of fluctuation is not significantly different from that at 5m; from 30m to 80m, the intensity of effective tension fluctuations decreases progressively, with the tension fluctuations being the most moderate at 80m, marking the point of least fluctuation along the entire cable; between 80m and 110m, the intensity of effective tension fluctuations begins to increase again; from 110m to 120m, the degree of fluctuation remains relatively stable; and from 120m to the seabed anchorage, the intensity of effective tension fluctuations decreases progressively.

From the perspective of fatigue damage, the greater the degree of fluctuation in effective tension, the higher the propensity for cables to suffer from fatigue damage and fracture. Consequently, the sections at 5m and 30m from the top end are identified as the most susceptible to fatigue fracture along the entire cable length. In contrast, the section at 80m from the top end is the least likely to experience fatigue fracture. Therefore, for the attachment of scientific instruments to the cable, this location is recommended as it minimizes the uncontrolled vibration of the instruments while ensuring their operational safety.

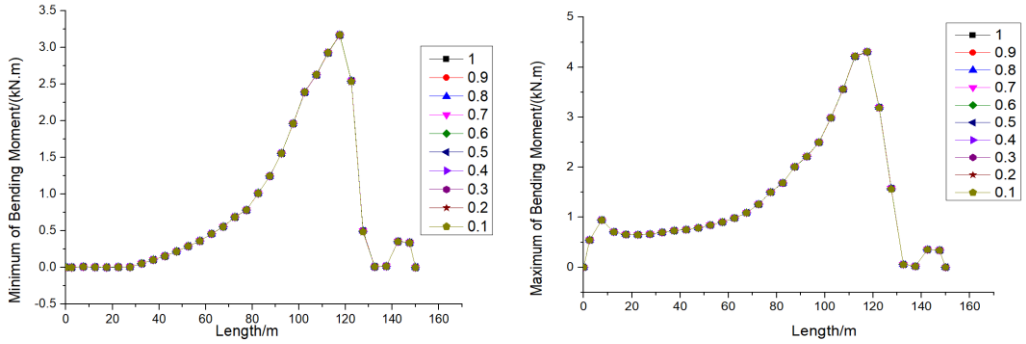

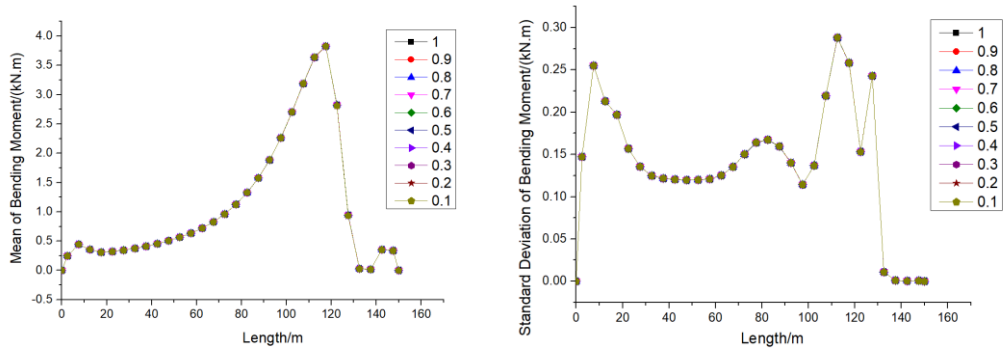

Figure.3. Bending Moment Variation of Cables with Different Poisson's Ratios.

From Figure 3,observations of the bending moment variations in cables under different Poisson's ratios indicate that changes in Poisson's ratio have a relatively minor impact on the bending moment of the cables. Comparing the distribution of the maximum, minimum, and average bending moments along the length of the cable under different Poisson's ratios reveals that, aside from slight numerical differences, the three curves exhibit a certain degree of similarity in shape along the cable length. The section of the cable that experiences the maximum bending moment is located 115 meters from the top end, with smaller bending moments at the top and anchor ends. Examining the changes in the standard deviation of the bending moment under different Poisson's ratios shows that within the length ranges of 30m-50m and 140m to the anchor end, the degree of fluctuation in the bending moment of the cable is relatively consistent, with the temporal variations in bending moment fluctuations being more synchronized in these regions. At distances of 10m, 110m, and 130m from the top end, the degree of fluctuation in the bending moment is more intense and the changes are more abrupt.

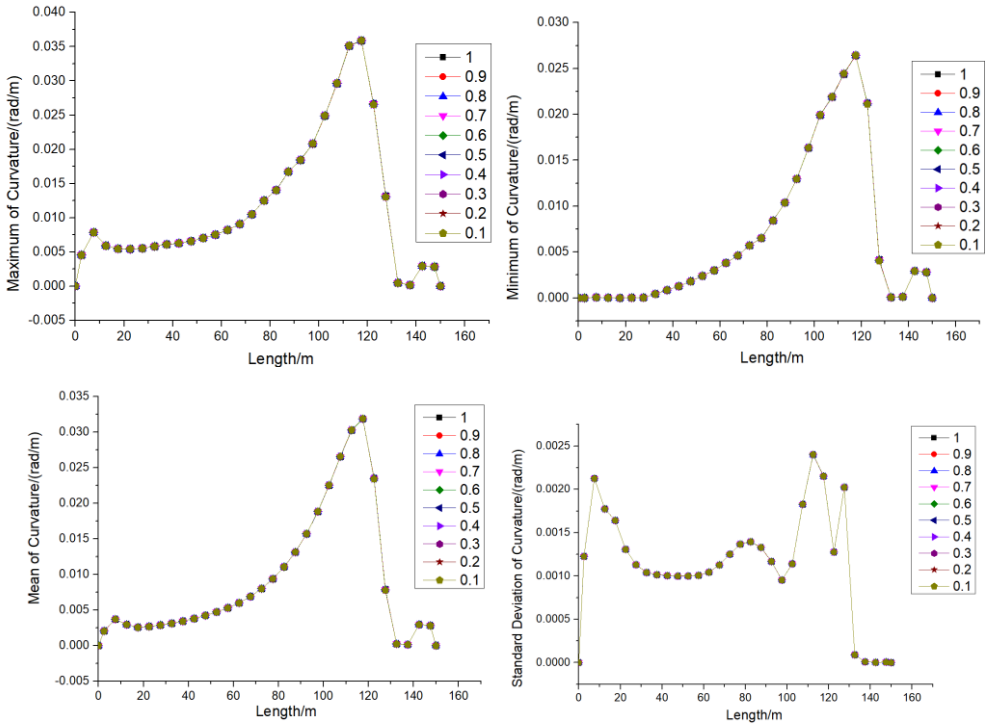

Figure.4. Curvature Variation of Cables with Different Poisson's Ratios.

As can be seen from Figure 4,upon examining the variation in bending moment of cables under different Poisson's ratios, it is observed that changes in Poisson's ratio exert a relatively minor influence on the curvature of the cables. A comparative analysis of the minimum values of bending moment and curvature, the maximum values of bending moment and curvature, and the average values of bending moment and curvature along the length of the cable under different Poisson's ratios reveals a high degree of morphological similarity among them. Further comparison of the distribution of the standard deviations of bending moment and curvature along the cable length under different Poisson's ratios indicates a certain degree of morphological similarity between the two. This suggests that the variations in bending moment and curvature are synchronous in the time domain, with no lag effect in force application and deformation.

4.2 The Impact of Linear Density on the Mechanical Performance of Mooring Cables

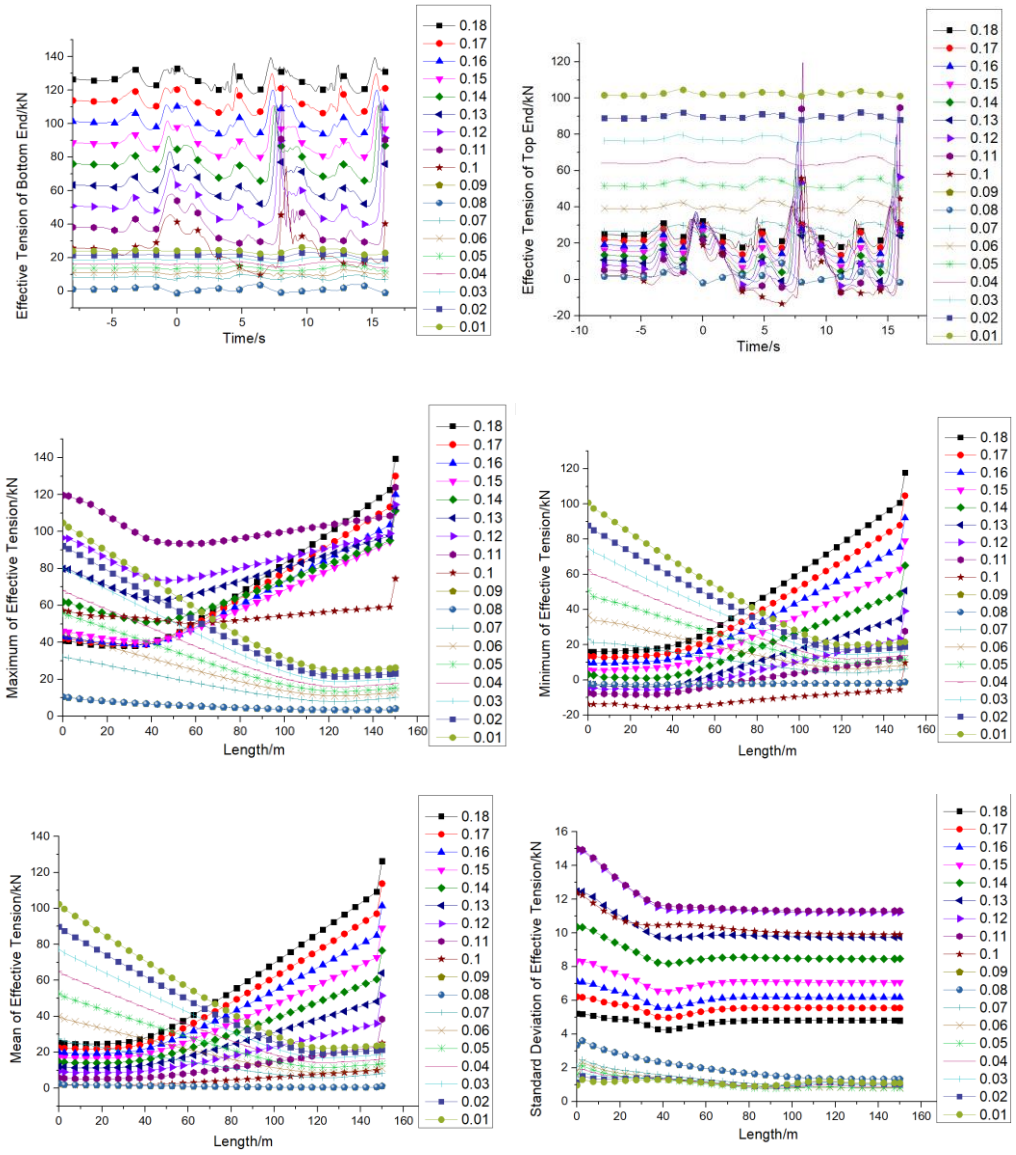

Figure.5. Variation in Effective Tension of Cables with Different Linear Densities.

From Figure 5, it can be seen that when observing the variation in the effective tension of cables with different linear densities, the change in cable linear density has a very significant impact on the magnitude of the cable's maximum effective tension. Observations of the effective tension at both ends of the cable over time reveal that when the linear density of the cable is low, the effective tension at the top end of the cable is greater than that at the bottom end. However, as the linear density continues to increase, the effective tension at the bottom end becomes greater than that at the top end. The reason for this phenomenon is analyzed as follows: when the linear density is low, the cable's mass is lighter, leading to greater deformation at the top end due to environmental loads, resulting in a more intense stretching effect and consequently a higher effective tension at the top compared to the bottom. As the linear density increases, the section of the cable experiencing the most intense stretching effect shifts from the top to the bottom, leading to a higher effective tension at the bottom end compared to the top end. The distribution of the maximum, minimum, and average values of effective tension along the cable's length further corroborates the validity of this conclusion.

Further examination of the distribution of the standard deviation of effective tension along the cable's length under different linear densities shows that the degree of fluctuation in effective tension decreases sequentially within the 0m-40m length range of the cable. Moreover, under different linear densities, the degree of fluctuation in effective tension remains stable from the 40m length to the anchor end. Changes in linear density have a noticeable impact on the degree of fluctuation in effective tension, with an initial increase followed by a decrease in the intensity of tension fluctuations as the linear density increases.

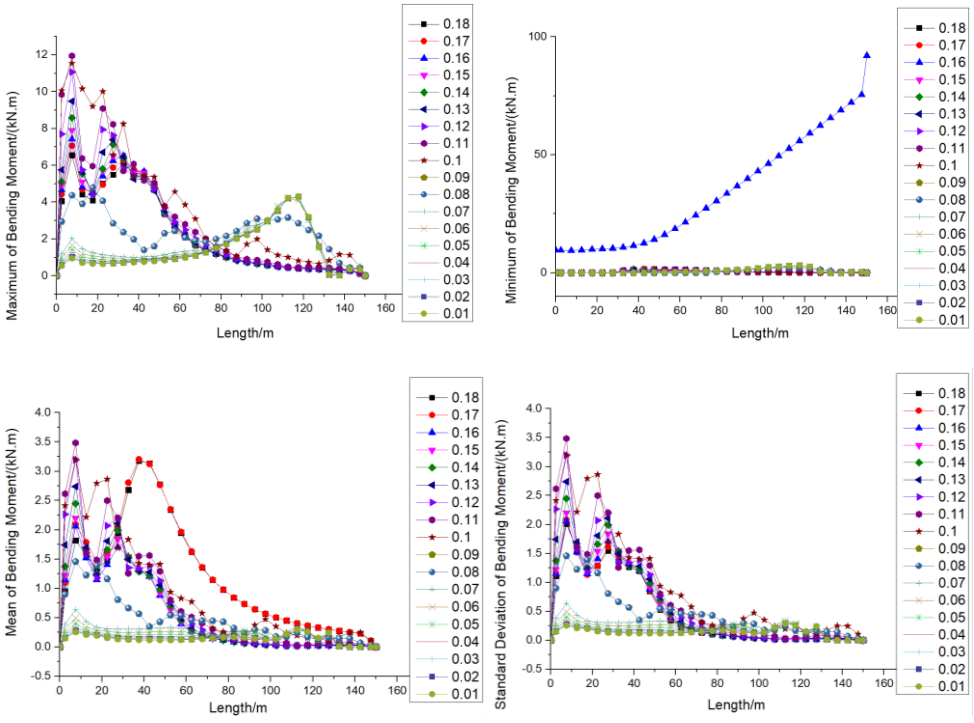

Figure.6. Variation in Bending Moment of Cables with Different Linear Densities.

Observing the variation in the bending moment of cables with different linear densities through Figure 6, it can be seen that the change in linear density has a relatively significant impact on the bending moment of the cables. The distribution of the maximum bending moment along the cable length suggests that the maximum bending moment initially increases and then decreases with an increase in linear density. The distribution of the minimum bending moment along the cable length indicates that, throughout the simulation time domain, when the bending moment at any position along the cable is at its minimum, the minimum bending moment at any location of the cable with a linear density of 0.16t/m is greater than the corresponding minimum bending moment at the same location for other linear densities. Further examination of the distribution of the minimum bending moment along the cable length with a linear density of 0.16t/m reveals that within the 0-40m length range, the minimum value of the cable bending moment remains constant; within the 40m-145m length range, the minimum value of the cable bending moment increases linearly; and within the 145m-anchor end length range, the minimum value of the cable bending moment increases sharply. For the remaining linear densities, the minimum bending moment along the cable length varies little and is essentially equal. The distribution of the standard deviation of the bending moment along the cable length under different linear densities indicates that as the linear density of the cable increases, the degree of fluctuation in the bending moment changes with the linear density, exhibiting a certain degree of randomness.

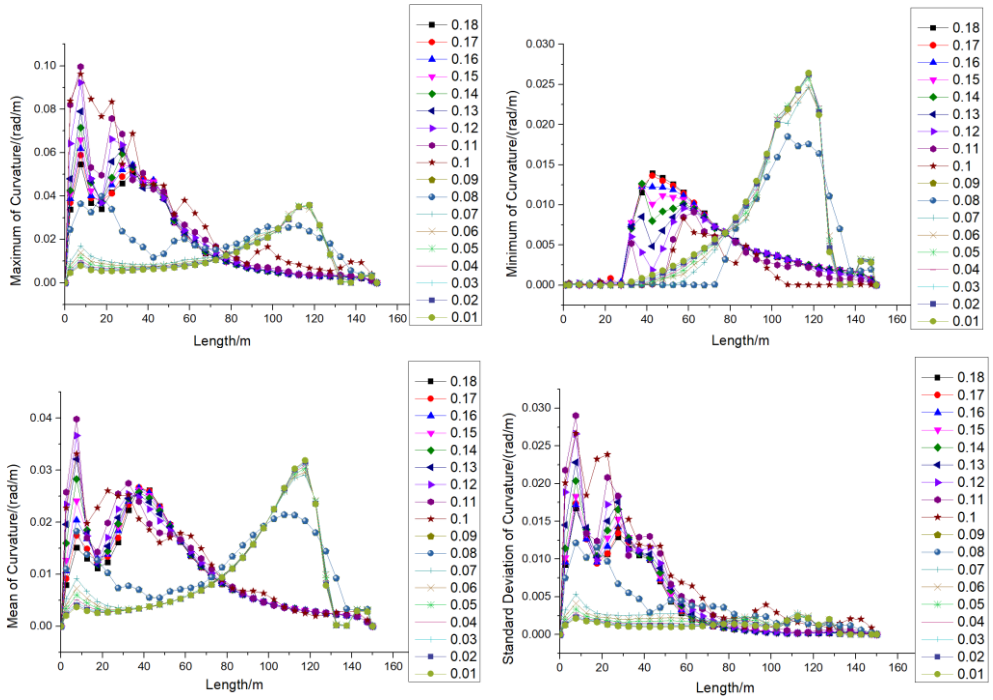

Figure.7. Curvature Variation of Cables with Different Linear Densities.

By comparing and observing in Figure 7 the variation in curvature and the distribution of bending moment variation along the length direction of cables with different linear

densities, it can be seen that as the linear density increases, there is a certain difference in the shapes of the two. This indicates that the changes in bending moment and curvature are not synchronous in the time domain, and there is a lag effect in force and deformation.

4.3The Impact of Elastic Modulus on the Mechanical Performance of Mooring Cables

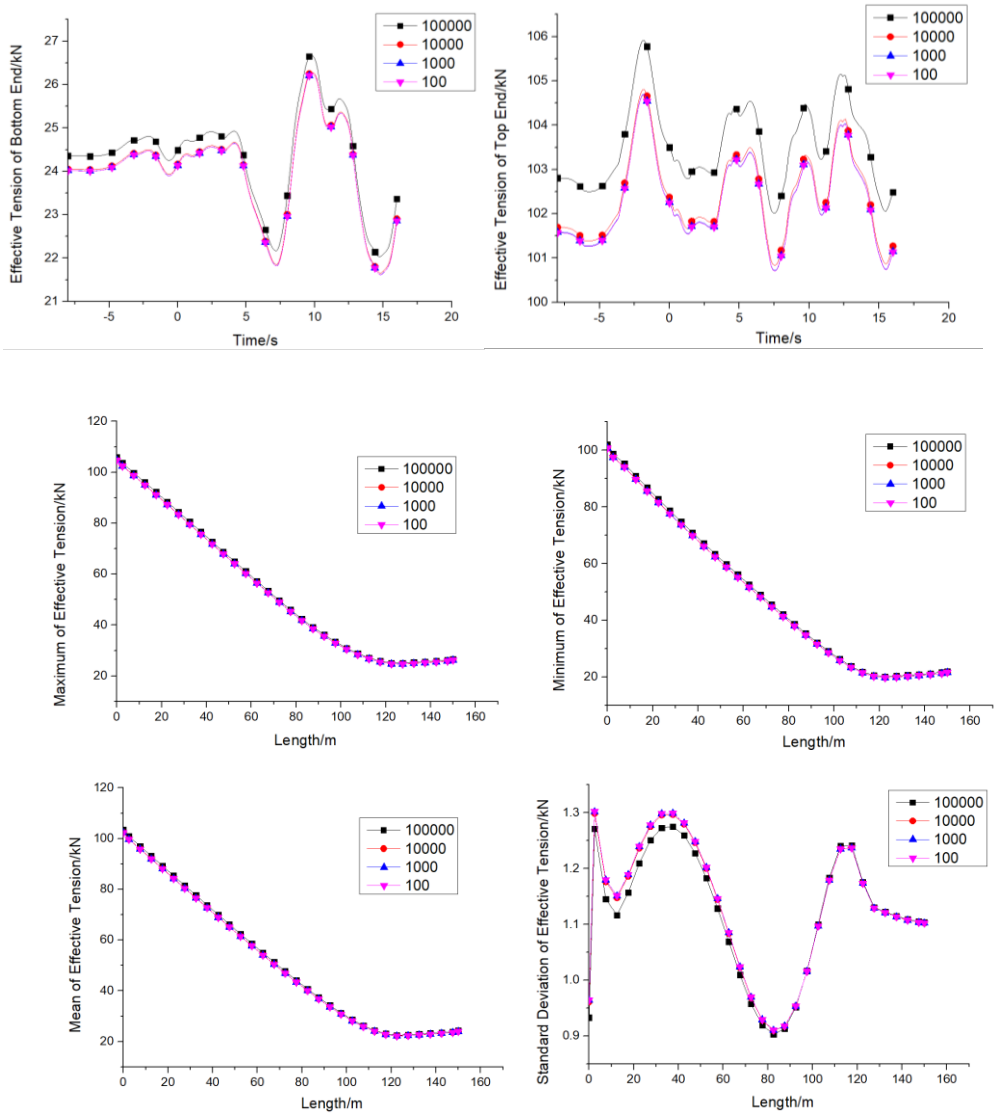

Figure.8. Variation in Effective Tension of Cables with Different Elastic modulus.

Observing the variation in the effective tension of cables with different elastic moduli in Figure 8, it can be seen that as the elastic modulus increases, there is a slight fluctuation in the effective tension of the cables, but the change is not significant.

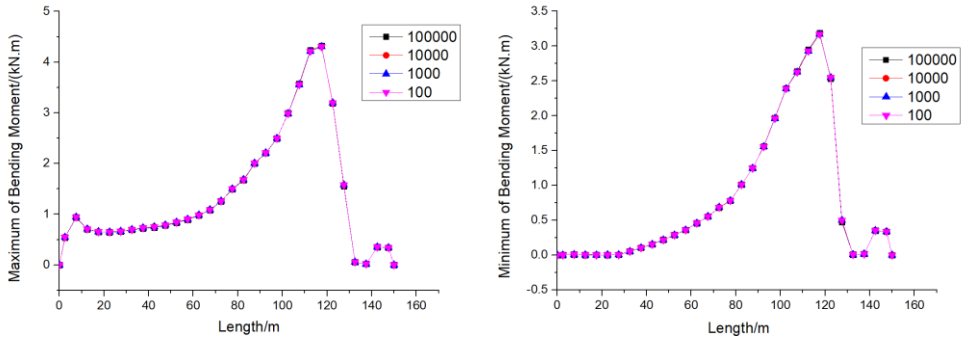

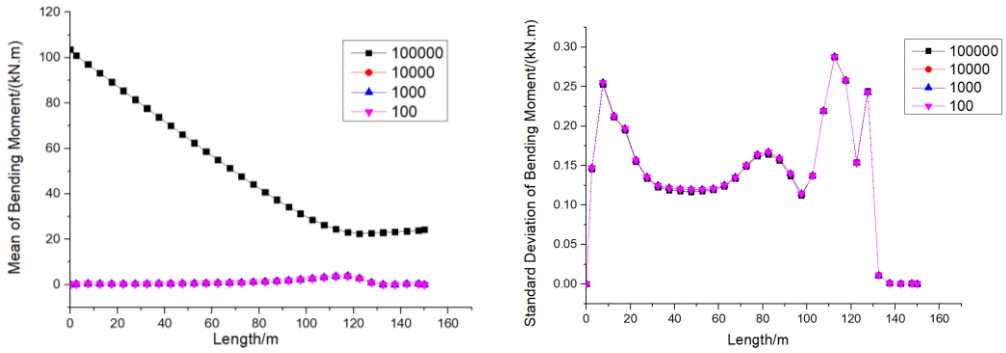

Figure.9. Bending Moment Variation of Cables with Different Elastic modulus.

Observing the variation in the bending moment of cables with different elastic moduli in Figure 9, it can be seen that as the elastic modulus increases, the maximum and minimum values of the bending moment that the cables can withstand remain essentially unchanged. However, when the elastic modulus is 100,000 Pa, there is a noticeable change in the average value of the cable bending moment. This indicates that when the elastic modulus increases to 100,000 Pa, the entire cable experiences a relatively larger bending moment in the time domain.

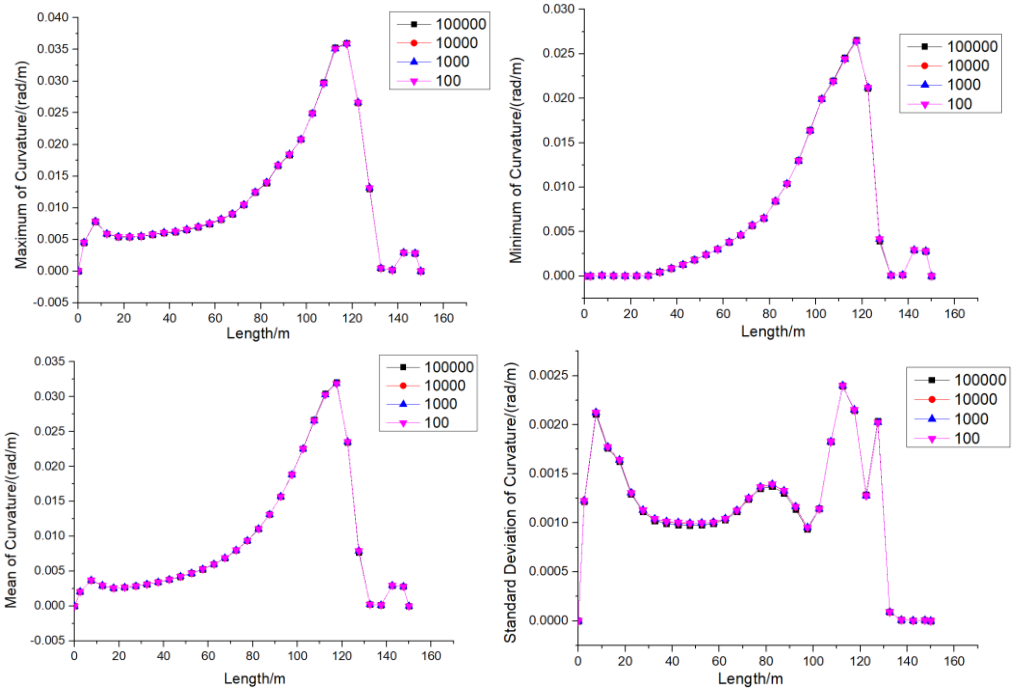

Figure.10. Curvature Variation of Cables with Different Elastic modulus.

Observing the variation in the bending moment of cables with different elastic moduli in Figure 10, it is observed that as the elastic modulus increases, the maximum, minimum, and average values of curvature along the length of the cable remain essentially unchanged. This suggests that the bending loads experienced by the cable and the resulting bending deformations are not entirely synchronous in the time domain, indicating a subtle lag effect between force application and deformation.

5. Conclusions

Observations regarding the variation in effective tension of cables under different Poisson's ratios reveal that changes in Poisson's ratio have a minimal impact on the effective tension of cables, with the curves of effective tension under different Poisson's ratios being highly coincident. Similarly, the influence of Poisson's ratio changes on the bending moment of cables is relatively minor. Variations in bending moment and curvature of cables under different Poisson's ratios are synchronous in the time domain, with no lag effect observed between force application and deformation.

Alterations in the linear density of cables significantly affect the changes in effective tension and bending moment of the cables. As the linear density increases, the variations in bending moment and curvature of the cables exhibit an asynchronous trend in the time domain, indicating a lag effect between force application and deformation. Changes in the elastic modulus (within 100–100,000 Pa) primarily influence the average bending moment of cables, as shown in Figure 9.

Among the variations in Poisson's ratio, linear density, and elastic modulus, changes in linear density have the most pronounced impact on the mooring mechanical characteristics of cables. The influence of elastic modulus changes ranks second, while changes in Poisson's ratio have the weakest effect on the mooring mechanical performance of cables.

References:

1. Breno Pinheiro Jacob, *et al*. Parallel implementations of coupled formulations fo r the analysis of floating production systems, Part II: Domain decomposition str ategies. Ocean Engineering. 2012; 55: 219-234.
2. Zhihua Ran. Coupled dynamic analysis of floating structures in waves and curre nt. Texas, College Station: Texas A&M University. 2000.
3. D. L. Garrett. Coupled analysis of floating production systems. Ocean Engineeri ng. 2005; 32(7): 802-816.
4. J. W. Kim, *et al*. Application of viscoelastic model for polyester mooring. Proce edings of the ASME 29th International Conference on Ocean, Offshore and Arct ic Engineering. Shanghai, China. 2010.
5. Fan Zhang, *et al*. Coupling effects for cell-truss spar platform: comparison of fr equency and time-domain analysis with model test. Journal of Hydrodynamics. 2 008; 20(4): 424-432.
6. Xiaoning Jing, *et al*. Coupled dynamic modeling of a moored floating platform with risers. Proceedings of the ASME 30th International Conference on Ocean, Offshore and Arctic Engineering. Rotterdam. Netherlands. 2011; 427-436.
7. Shan Ma, *et al*. Asynchronous coupling analysis of dynamic response for deepw ater moored floating. Proceedings of the 8th International Workshop on Ship Hy drodynamics. Seoul, Korea. 2013.
8. Shan Ma, *et al*. Asynchronous coupled analysis of a single point moored FPSO. 10th International Conference on Hydrodynamics. Petersburg, Russia. 2012.
9. Shan Ma, *et al*. Dynamic asynchronous coupled analysis and experimental study

for a turret moored FPSO in random seas. Journal of Offshore Mechanics and Arctic Engineering. 2015; 137(4): 6-10.

10. Sangsoo Ryu, *et al*. Prediction of deepwater oil offloading buoy response and e xperimental validation. International Journal of Offshore and Polar Engineering. 2006; 16(4): 290-296.
11. Y. M. Low, *et al*. A hybrid time/frequency domain approach for efficient couple d analysis of vessel/mooring/riser dynamics. Ocean Engineering. 2008; 35: 433-4 46.
12. Yihua Su, *et al*. Experimental study on dynamics of largely truncated mooring l ines. Journal of Ship Mechanics. 2010; 14(9): 967-976.
13. Arcandra Tahar, *et al*. Coupled-dynamic analysis of floating structures with poly ester mooring lines. Ocean Engineering. 2008; 35: 1676-1685.
14. Yong Bai, *et al.* Dynamic analysis of umbilical cable under interference with ris er. Ships and Offshore Structures. 2018; 13(8): 809-821.
15. Standards Belgian. Petroleum and natural gas industries — Specific requirements for offshore structures — Part 7: Stationkeeping systems for floating offshore structures and mobile offshore units. AS ISO 19901-7. 2019.
16. Smith J, *et al.* Experimental validation of mooring cable dynamics under wave l oads. Ocean Engineering. 2022; 210: 108-120.